and 26% for the (220) structure factors of the copper data. Because of the restriction $r^*_{Cu} \geq r^*_{Mo}$ it is clearly impossible to obtain a self-consistent interpretation of the combined copper and molybdenum data without taking the Borrmann effect into account.

It is a most surprising result to find such a high degree of perfection (as illustrated by the large values for r and g) for a crystal which has been ground into a sphere. The pure extinction effect is very great for both radiations firstly because r^* is large, and secondly because of the simplicity of the structure which allows F_c/V to be very large for many reflections. For the same two reasons, with the additional condition $\mu_0 R \gg 1$, the Borrmann effect becomes very great for the copper data.

The good agreement between theory and experiment suggests that the intensity formula presented in the preceding paper is satisfactory even for extreme conditions of extinction. However, further experimental tests of the theory are needed.

The writer is deeply indebted to Miss H.A.Plettinger, who made most of the intensity measurements. The work was in part supported by the Advanced Research Projects Agency under Contract SD-89.

References

ABRAHAMS, S. C., ALEXANDER, L. E., FURNAS, T. C., HAMILTON, W. C., LADELL, J., OKAYA, Y., YOUNG, R. A. & ZALKIN, A. (1967). *Acta Cryst.* **22**, 1.
CROMER, D. T. (1965). *Acta Cryst.* **18**, 17.
CROMER, D. T. & WABER, J. T. (1964). Los Alamos Scientific Laboratory Reports, LA-3056.
ZACHARIASEN, W. H. (1968). *Acta Cryst.* A**24**, 421.

Acta Cryst. (1968). A**24**, 427

Diffraction of Light by Opals

BY J. V. SANDERS

Commonwealth Scientific and Industrial Research Organization, Division of Tribophysics, University of Melbourne, Australia

(*Received* 20 *December* 1967)

Gem opals were examined in an optical diffractometer and found to give several types of diffraction pattern which are interpreted by analogy with conventional three-dimensional X-ray theory to give the structure of the opal. The results show that the spherical silica particles in opals are arranged hexagonally in layers which are usually stacked randomly. In some specimens there are parallel domains of ordered packing, commonly in a f.c.c. sequence and sometimes in a h.c.p. sequence. Although the silica particles cannot be resolved by optical microscopy, bands parallel to the layers and fringes across the bands can be seen in images with the diffracted light.

Introduction

Precious opal is an unusual form of silica and is valued as a gemstone because it exhibits intense colours which come and go or change in wavelength as the gemstone is viewed at various angles in white light. It is this effect of the play of colours which gives opals their distinctive appearance.

This property has not been well understood (Leechman, 1961). Baier (1932) made extensive optical measurements on opals, and suggested that opal was a pseudomorph of calcite (Baier, 1966) and that the colours arose by diffraction from regularly spaced sets of planes which originated in the twinned structure of the calcite. Raman & Jayaraman (1953) as well as Baier (1932) noted the high degree of monochromatism in the colour; they realized that this must be due to diffraction, and suggested an arrangement of equally spaced parallel plates of two forms of silica of different refractive indices.

It has recently been shown by Jones, Sanders & Segnit (1964) that precious opals are composed of spherical particles of amorphous silica whose size (1500–3500 Å) is too small for their resolution in an optical microscope, but large enough for them to be easily visible in an electron microscope. In gem quality opal the particles are remarkably uniform in size and they were therefore able to pack together regularly to form a pseudo-crystal. The particles of silica are transparent to light, but the unfilled voids between them scatter light because of the change of refractive index at their interfaces. This arrangement makes a three-dimensional grating which can give diffracted beams of light in the visible range when the particles of silica are larger than about 1500 Å in diameter (Sanders, 1964).

Electron microscopy clearly reveals the ordered arrangement of voids at the surface of opals, but the technique is not very suitable for investigating the packing arrangement of the particles of silica, because

of the random nature of the fracture surfaces and the lack of natural faces to assist in orienting the specimens. Furthermore, one can determine only the packing in the surface of very small samples of the opal. By contrast, optical diffraction should give information about the average structure throughout a specimen. An optical diffractometer was therefore set up and diffraction patterns obtained from many specimens mostly from Australian mines. Most of the observations were made visually, but some of the diffraction patterns were recorded photographically on black and white or colour film.

Several types of optical diffraction patterns from opals will be described, and their interpretation given by analogy with the X-ray case. This gives the packing arrangement of the silica particles, or what we call the opal structures. Some relevant features of the appearance of opals in optical and electron microscopes can then be related to these structures.

Experimental

The optical diffractometer (Fig. 1) consisted of a light source (L), a collimating lens (C) and a glass flask (F) in which the opal was mounted. For quantitative work a mercury–cadmium lamp was used as a source of light, giving spectral lines of known wavelength throughout the visible band. However, since there is a wide variation in intensity of the different colours from spectral lamps, a filament lamp giving a continuous spectrum was found to be more suitable for qualitative observations and for photography.

The opal specimen (O) was mounted at the centre of the flask (F) on one end of a goniometer (inset Fig. 1), and could be rotated about two perpendicular axes through its centre. Orientations were measured on the two graduated circles P_1 and P_2. The flask was filled with dekalin – an inert, transparent fluid whose refractive index is close to that of silica. Thus chips of opal of any shape could be used, without refraction at their surface interfering with the observations. Light entered the flask through an optical window (W, *ca.* 1 cm^2) cemented onto the outside of the flask. The divergence of the light was controlled by an aperture in front of the collimating lens.

For visual observation, the glass flask was spherical, and was coated on the outside with translucent paint to make a screen. For photographic recording, a transparent cylinder was used, the film being wrapped around the outside with a layer of dekalin between it and the glass to minimize scattering of light at the interfaces. A hole in the film allowed light to enter the vessel. Both colour positive (Ektachrome type B) and black and white (Ilford FP3) sheet films were used.

Several hundred chips of opal were inspected by eye, and a selection made of those whose appearance indicated that they were single grains. Most of the samples came from the mines at Andamooka or Coober Pedy in South Australia, but a few samples from other sources were also examined. These chips were generally irregularly shaped and a few mm in size. They were cemented onto a blackened holder which was attached to the goniometer, and then lowered into the flask and positioned at its centre in the beam of light.

Diffraction results

The diffraction patterns were easily visible on the screen in a darkened room, and consisted of streaks and separate spots of colour in the back-diffraction region. The positions and colours of these spots and streaks changed systematically as the opal was rotated. The wavelength of the colour increased with diffraction angle and was a maximum when the rays were diffracted back into the incident direction, *i.e.* when the Bragg angle, $\theta = \pi/2$. In a typical pattern red features appeared near the entrance window and the other spectral colours were dispersed in order of decreasing wavelength over an angle of about 90°, so that violet appeared at the sides of the flask. Fig. 2 shows two typical diffraction patterns recorded on colour film; one is with a filament lamp as source [Fig. 2(a)] and the other with a spectral lamp [Fig. 2(b)]. In the single streak in Fig. 2(a) the incident white light is dispersed into a line spectrum symmetrically about its centre (the black disc is the entrance window and the orange smear on the left hand side of it is an artifact produced by some scattered light). These colours all changed to longer wavelengths as the streak approached the window, and systematically to shorter wavelengths when the opal was rotated away from this position. In Fig. 2(b) discrete wavelengths lie on the streak SS', and there is an isolated spot at P.

Since the maximum wavelength which can appear by diffraction is related to the size of the silica particles in the opal (Sanders, 1964), the upper limit of wavelength in the diffraction patterns varied between specimens. For convenience, most measurements were made on specimens for which this limit was in the red end of the spectrum, *i.e.* where the particles were large enough to give all colours of the visible spectrum. Generally, the results and their interpretation are quoted in terms of these specimens, but they apply in principle also to specimens giving a more restricted range of colours.

Many samples gave indistinct patterns, presumably due to distortions or mosaic structures within the grain. Measurements were therefore restricted to those samples which gave clear, unambiguous patterns.

To obtain complete diffraction information from a sample, it was rotated through all angles and the orientations recorded when it was in positions giving diffraction back into the incident beam direction, *i.e.* when the Bragg angle was $\pi/2$ and the Bragg relationship became $n\lambda = 2d\mu$, where d is the interplanar spacing, μ the refractive index of opal, and λ the wavelength, in air, of the colour which was back-diffracted. These orientations were plotted stereographically on a

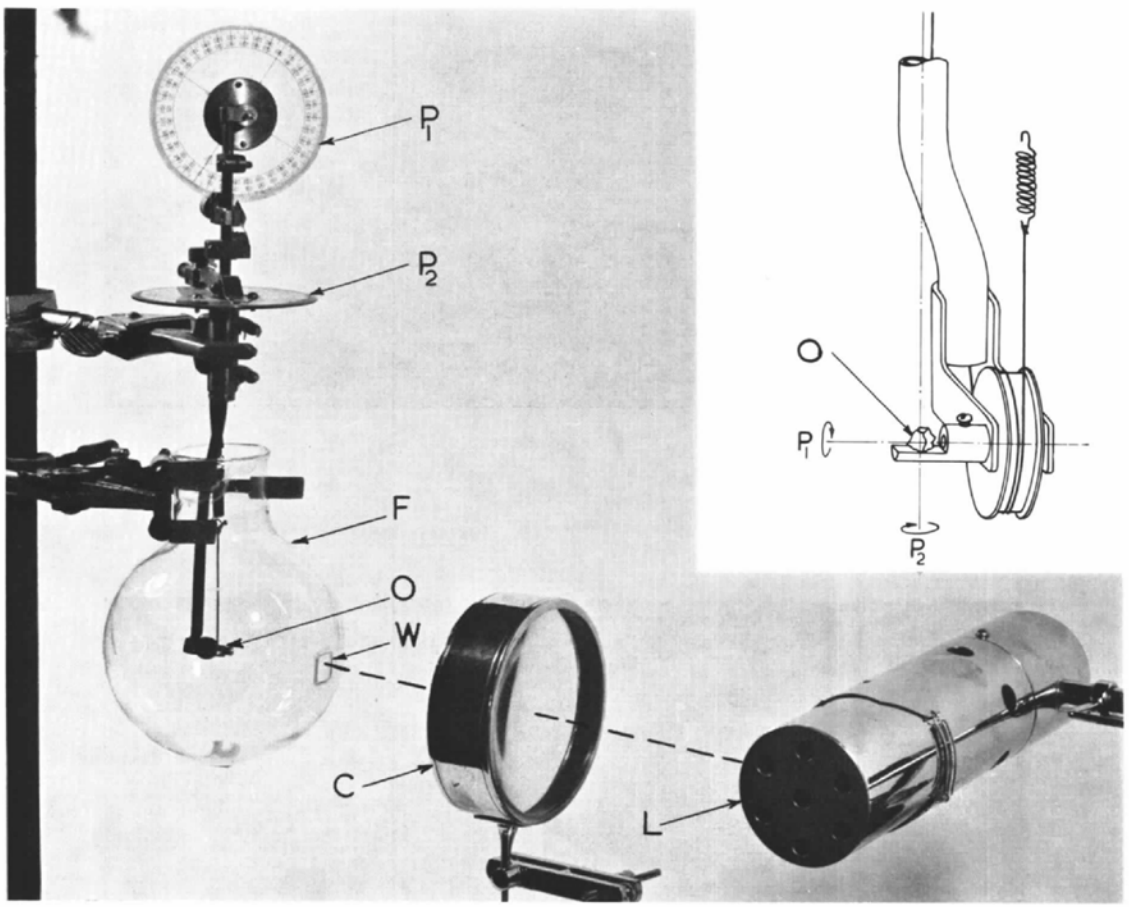

Fig. 1. Optical diffraction apparatus: *L*, spectral lamp; *C*, lens; *F*, flask; *W*, entrance window; *O*, opal specimen; P_1, P_2, graduated circles for reading orientations: inset, details of mounting of opal on goniometer. The flask was photographed uncoated to show details of the goniometer.

[*To face p.* 428

(*a*)

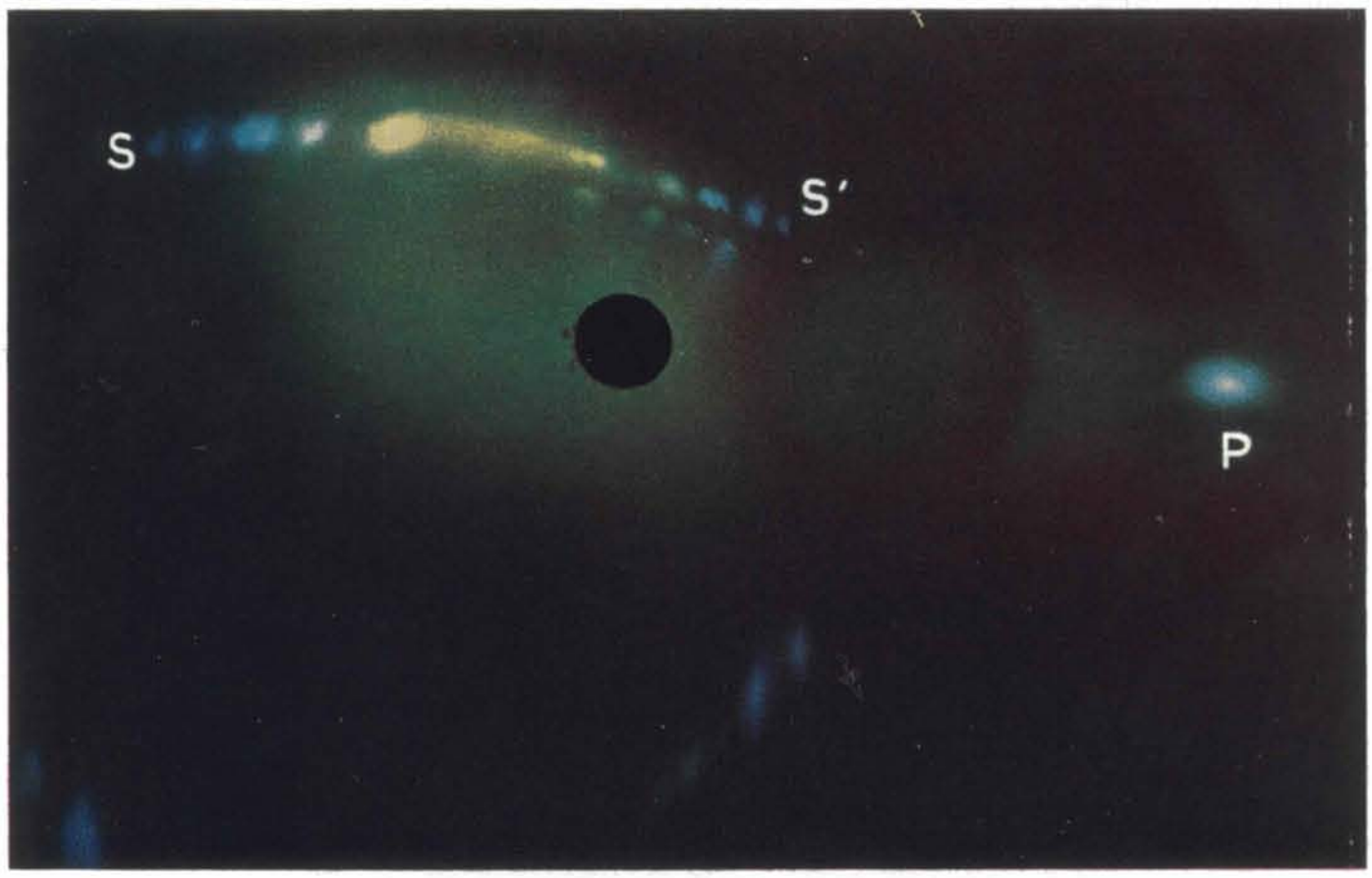

(*b*)

Fig. 2. Diffraction patterns recorded on colour film bent around a cylindrical flask. The light sources were (*a*) tungsten filament lamp, (*b*) Hg–Cd spectral lamp.

Wulff net to give a projection of all the back-diffracting positions of the opal relative to the direction of incidence of the light, except a small range of angles which were obscured by the holder. Because the samples were mounted without regard to their orientation, these stereograms generally showed no symmetry. They were therefore replotted by transposing one of the isolated diffraction spots to the centre of the stereogram, and then symmetry appeared. In the discussion which follows, only such transposed stereograms are considered.

Several different types of diffraction patterns were distinguished and they and the stereograms were therefore divided into four categories.

I. The most common type of pattern contained two spots (subsequently called poles) and some sharp streaks, along which the colours changed in spectral order decreasing in wavelength on both sides of the centre of the streak. Fig. 2(*a*) is an example of one of these streaks, in which the longest wavelengths in the centre are in the infrared, and hence are not visible. Stereograms, replotted with one of the poles at the centre of the stereogram (Fig. 3) contained six streaks radiating symmetrically about the pole with the colour changing from a maximum wavelength at the equator, through the spectral series to the shortest visible wavelength as it approached the pole. The colour at the equator was always of slightly longer wavelength than that of the isolated pole, *e.g.* typically they were red and orange respectively.

The sixfold symmetry of the stereogram was not generally apparent in the diffraction patterns. However, if a specimen was mounted so that the two poles were on the vertical axis of the goniometer, vertical streaks of colour appeared and followed one another at 60° intervals as the opal was rotated about its vertical axis.

Frequently, there was no obvious intensity variation along the streaks, but this has not yet been measured.

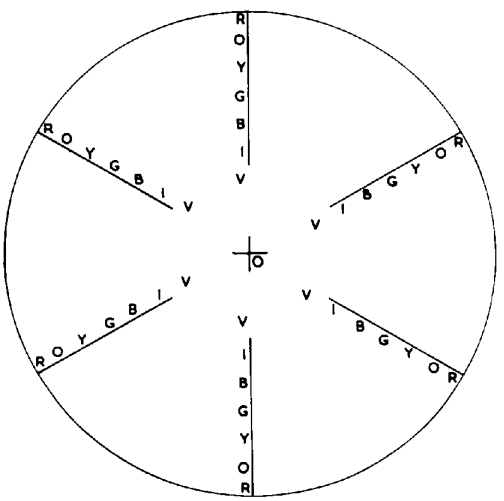

Fig. 3. Stereogram I. The letters *V*, *I*, *B*, *G*, *Y*, *O*, *R* indicate colours of the spectrum (violet, indigo, blue, green, yellow, orange, red).

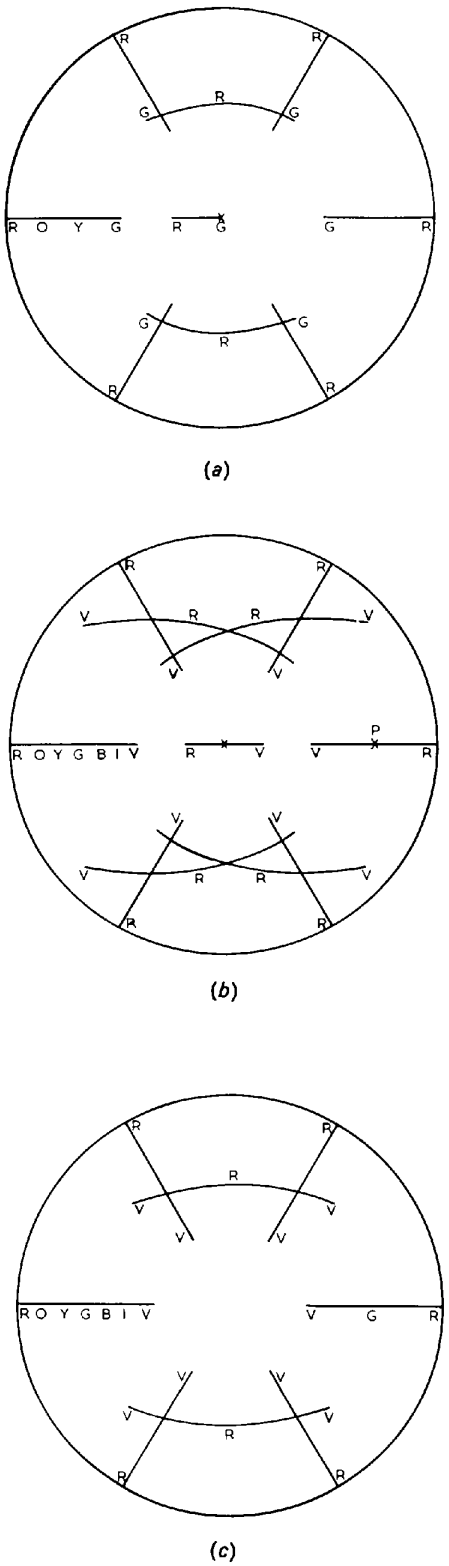

Fig. 4. Stereograms of intersecting streaks; (*a*) observed (*b*), (*c*) predicted for twinning of type I structures. The wavelengths of colours change continuously along the streaks, from the extremes shown (*R*, red; *G*, green, *etc.*); *X* is a pole.

Some patterns containing marked variations of intensity are considered separately in III.

II. A few specimens gave patterns containing streaks which intersected at a common colour, and with the same arrangement of colours. Fig. 4(*a*) is a stereogram of such a pattern, replotted with a pole at the centre of the stereogram. The arrangement of the colours in the streaks and poles was the same as for I. Fig. 4(*b*) and (*c*) are theoretical, and will be discussed later.

III. In a few cases there were spots superimposed on the streaks, or the streaks were broken into intensity maxima. In the diffraction patterns a maximum of intensity sometimes occurred at the position of maximum wavelength of a streak in its back diffracting position (positions *R* on the stereogram, Fig. 3), but more frequently they were symmetrically placed about that position. The colours of the spots were the same as that of the streak at that point.

IV. The simplest diffraction patterns consisted only of sharp spots of colour. One of the few samples in this group was a glassy chip, roughly a 2 mm cube, giving the stereogram in Fig. 5 which is plotted with one of the spots at the centre. Several other chips gave similar stereograms. Only two colours occur in the back-diffracted positions: in the sample giving Fig. 5 they were red and lime-green (visual estimate $\lambda_R = 7000$ Å, $\lambda_{LG} = 6000$ Å) respectively.

Interpretation

Electron microscopy has shown that the silica particles are spheres of uniform size, and micrographs like Fig. 6 have established that they are arranged in nearly perfect hexagonal arrays in layers. We are now concerned with determining the stacking sequence of these layers from the diffraction patterns and stereograms. We will usually choose a hexagonal set of axes within a layer, parallel to the close-packed rows, and a *C* axis perpendicular to the layer. Close-packed layers of particles of radius *r* are equally spaced with a separation $c = r^2\sqrt{8/3}$. At times we will treat these layers as (111) layers in a f.c.c. structure and index accordingly.

Guinier (1963) considered the various ways in which such layers of particles may be arranged, and calculated the reciprocal lattices for various stacking sequences. When the layers are randomly stacked, their reciprocal lattice consists of infinite rods parallel to **C*** and passing through *hki*0 except when $h-k=3n$; in the latter case the rods are replaced by a series of points with a spacing $1/c$. The part which is accessible to light in the visible spectrum is restricted to the six rods passing through the points $10\bar{1}0$ and the two points at 0001 and $000\bar{1}$ as shown in Fig. 7. Guinier shows that the intensity of scattering of X-rays oscillates along the rod with minima at $10\bar{1}l$ ($l=2n$) of one ninth that of the maxima in between.

If the stacking sequence of the layers is regular, it may give a h.c.p. structure (conventionally, stacking sequence *ABABAB*...) or f.c.c. (stacking sequence *ABCABC*...). In these cases the reciprocal lattices contain only points, some of which are shown at positions *H* in Fig. 8 for h.c.p., and at *C* for a f.c.c. structure.

Type I

If light is scattered at the surface of the particles, and they are packed like hard spheres, the scattering lattice is the same as that of the particles. Reciprocal lattice geometry used for X-ray diffraction is applicable here because the planes of particles in gem opals have spacings similar to the wavelengths of light in the visible region. Fig. 9 shows how a reciprocal lattice rod produces a streak of colour. This is a section through the Ewald spheres for light, incident from the top, containing the colours violet (*V*), blue (*B*), green (*G*), yellow (*Y*), orange (*O*), red (*R*). *QQ'* is one position of a reciprocal lattice rod and *P* a reciprocal lattice point corresponding to a pole. The rod *QQ'* splits the incident light into a line spectrum consisting of colours in directions away from the centres of the corresponding Ewald spheres, *i.e.* in the directions *OO'*, *YY'*, *GG'*, *BB'*, *VV'*. Thus the wavelength decreases on each side of a maximum wavelength *O*. However, the point *P* gives only one diffracted colour in the direction shown

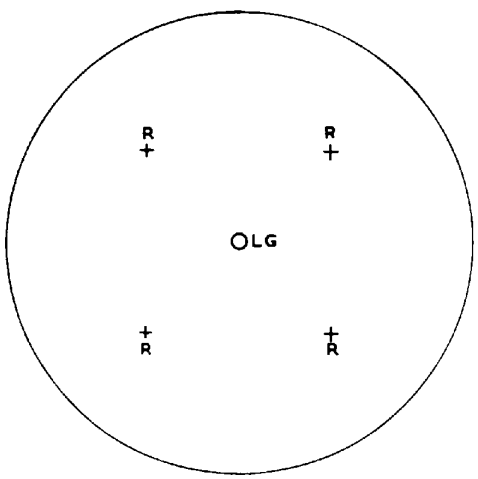

Fig. 5. Stereogram IV: *R*, red, *LG*, lime-green.

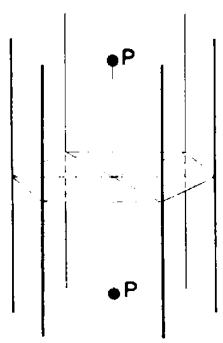

Fig. 7. Part of the reciprocal lattice of randomly stacked layers with hexagonal symmetry.

in the diagram. This situation is appropriate for the diffraction pattern in Fig. 2(*b*), where the diffracted beams lie on a streak *SS'*, which is curved because of the geometry of the optical arragement. This diagram (Fig. 9) also shows how the colours should change if the opal is rotated about an axis through the origin perpendicular to the page, because as *P* moves along the arc *P'P''*, it cuts Ewald spheres of decreasing radius and hence gives diffraction colours of increasing wavelength, which reach a maximum at *P''*, when the opal has the orientation in Fig. 10(*b*). At the same time the reciprocal lattice rod *QQ'* shifts, *N'N''* being its envelope, and the diffraction colours decrease in wavelength. It is clear that the colour of maximum wavelength which can be seen in a streak occurs when the reciprocal lattice rod passes through *N'*, *i.e.* when it is perpendicular to the direction of incidence of the light, in the situation shown in Fig. 10(*a*). Then the colours appear symmetrically displaced about the longest wavelength. The streak in Fig. 2(*a*) is slightly displaced from this position.

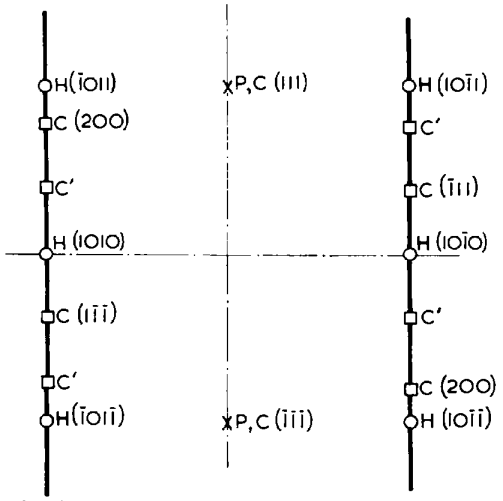

Fig. 8. Section through reciprocal lattice showing effect of regular stacking in cubic (*C*, *C'*) or hexagonal (*H*) sequence.

Visual observation confirmed that the individual streaks and spots of colour in patterns of type I behaved in this way, and it can be concluded that they come from straight reciprocal lattice rods and points respectively. The sixfold symmetry of the stereograms

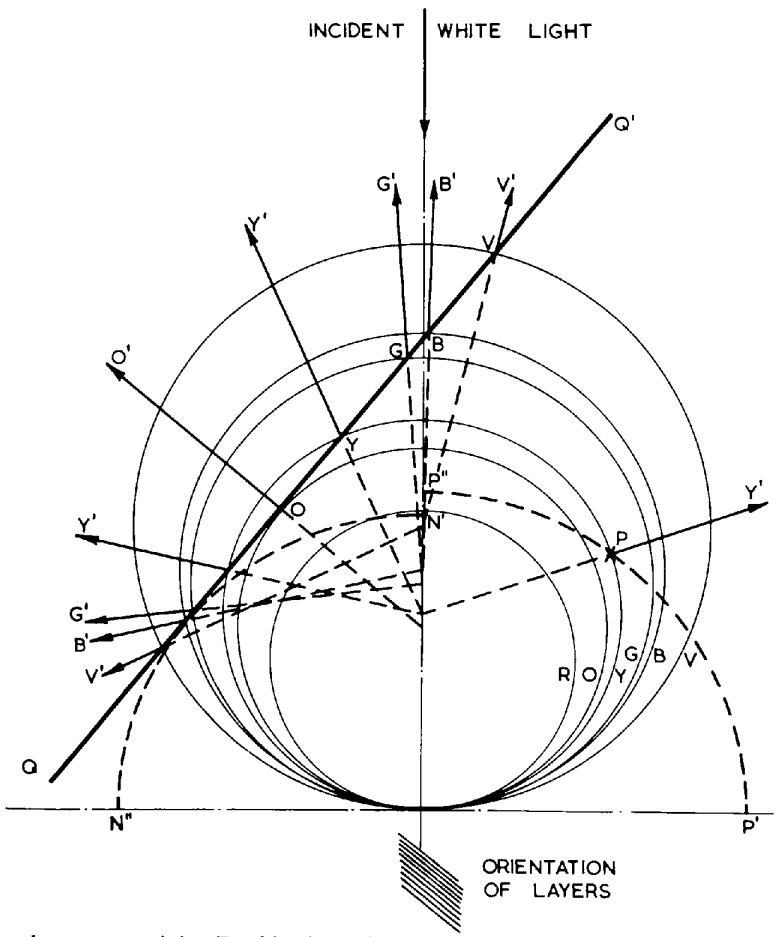

Fig. 9. Section of reciprocal space containing Ewald spheres for violet (*V*), blue (*B*), green (*G*), yellow (*Y*), orange (*O*), and red (*R*) light. The reciprocal lattice rod *QQ'* produces a streak of colours and the pole *P*, a spot of colour if white light is incident from above.

I is consistent with the reciprocal lattice arrangement shown in Fig. 7. Furthermore, the wavelengths of the colours which appear at special positions can be related to the spacing of diffracting planes. The reciprocal lattice positions at which colours given by streaks and spots reach their maximum wavelengths (λ^s_{max}, λ^p_{max} respectively) are shown in Fig. 10(*a*) and (*b*). The longest wavelength in the streaks (equivalent to diffraction from $(10\bar{1}0)$ planes in a h.c.p. structure) is

$$\lambda^s_{max} = 2\mu r/\sqrt{3} ,$$

and that of the poles (when it is in the position P'', Fig. 9, equivalent to diffraction from (111) planes in a f.c.c. structure) is

$$\lambda^p_{max} = 2c\mu = 4\mu r 2/\sqrt{3} .$$

Thus

$$\lambda^p_{max}/\lambda^s_{max} = 2\sqrt{2}/3 = 0{\cdot}94 .$$

This accounts for the observation that the poles of the stereograms have colours of slightly shorter wavelength than that of the longest wavelength in the streaks.

Thus the symmetry of the stereogram and the positions of colours of various wavelengths in it are consistent with the reciprocal lattice in Fig. 7. It is concluded therefore that in the specimens giving patterns of type I, the particles are arranged hexagonally in layers, and the layers are stacked in a random sequence.

Type II

Patterns containing intersecting streaks seem to be due to twinning on some plane inclined to the layers. The stereograms which would be produced by twinning a randomly stacked structure in two different ways are plotted in Fig. 4. If the layers were parallel to one of the {111} planes in a cubic structure, and the twin planes were parallel to another of the {111} planes, the stereograms become Fig. 4(*b*). If the twin plane were $(10\bar{1}0)$ of a h.c.p. structure in which the layers were parallel to (0001), Fig. 4(*c*) should occur. The observed stereogram, (*a*), is consistent with (*c*) but not (*b*). Thus this specimen is twinned on a plane normal to the layers, and parallel to a row of particles.

Type III

The positions of intensity maxima can be shown to occur at positions on the streaks corresponding to the points *C*, *C'*, *H* on the reciprocal lattice rods in Fig. 8. The position $H(10\bar{1}0)$ is easily recognizable because it coincides with the centre of the streak when the sample is in the position shown by Fig. 10(*a*). Intensity maxima at the positions *H* indicate the presence of domains ordered in a h.c.p. manner.

The positions of the other maxima were measured with respect to this position, and found to coincide with the other marked points. In Fig. 8 the points *C* come from a f.c.c. structure equivalent to a single crystal giving a 111 reciprocal lattice point at the pole, *P*. Twinning on the plane parallel to the layers would produce intensity maxima at the positions marked *C'*. Observation showed that when intensity maxima occurred at positions *C*, there were equally intense maxima at positions *C'*. Therefore such specimens contain domains in which the layers are packed in a f.c.c. sequence but the two possible senses (twin arrangements) occur with equal probability. Thus these specimens can consist of randomly stacked layers containing ordered domains with the f.c.c. stacking sequence *ABCABC*... or *CBACBA*..., sometimes together with the hexagonal sequence *ABAB*...

As yet the number of samples examined is insufficient to give useful estimates of the relative frequency of occurrence of the various forms, or to relate them to the source of the sample.

Type IV

The absence of streaks in these diffraction patterns implies that there is no disorder in the structure. The positions of the spots in the stereograms are consistent with the angles between (100) and (111) planes in a cubic structure. The wavelengths of the colours in the stereogram are 7000 Å and 6000 Å, so that the spacings of the diffracting planes are 2400 Å and 2100 Å ($\mu = 1{\cdot}45$). The ratio of the spacings of (200) and (111) planes is $d_{200}/d_{111} = 4/\sqrt{3} = 1{\cdot}15$, which is consistent with the ratio of the wavelengths of the colours and identifies the structure as f.c.c.

Electron microscopy

It has not yet been possible to obtain systematically electron micrographs of sections whose orientations have been determined by optical diffraction, and so confirm the structures directly. However, many of the micrographs from random fracture surfaces show significant features such as the sixfold symmetry in Fig. 6. Domains of cubic packing could be seen in sections such as Fig. 11, and would suggest that this sample belonged in category III. This is a section passing through the close-packed rows in $[11\bar{2}0]$ directions, and inclined at 59° to the layers. This field contains a do-

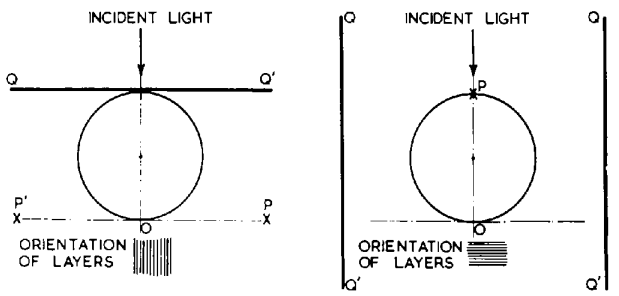

(*a*) (*b*)

Fig. 10. Relative orientations of layers and reciprocal lattice in positions giving (*a*) colour of maximum wavelength in a streak, (*b*) colour of maximum wavelength at a pole. The circle is a section through the Ewald sphere for the colour of maximum wavelength; *QQ'* a reciprocal lattice rod; *P*, a pole.

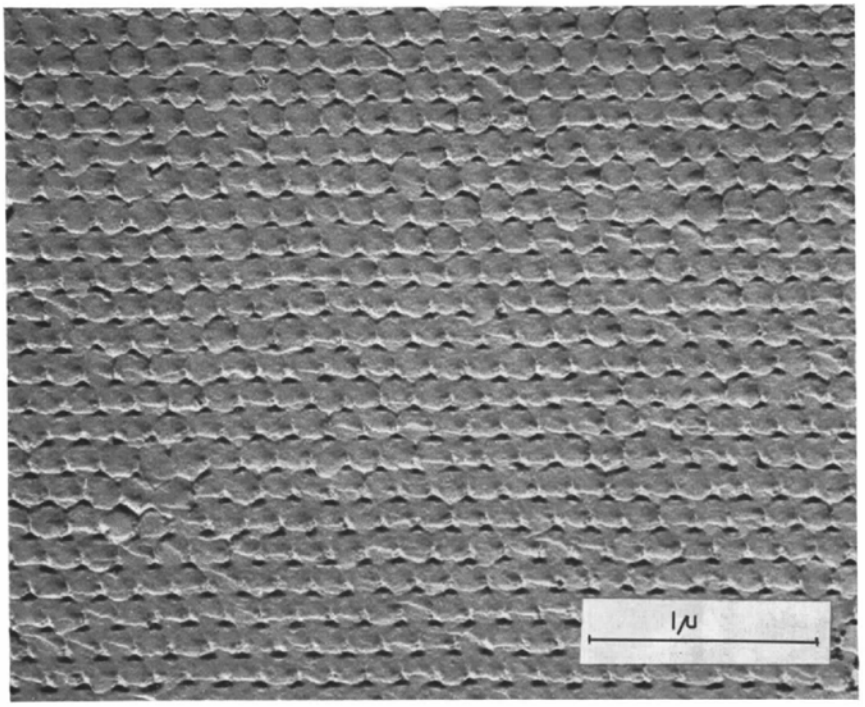

Fig. 6. Electron micrograph of a replica of the fracture surface of gem opal. This regularity of packing extends over a much larger area than the field shown here (× 30,000).

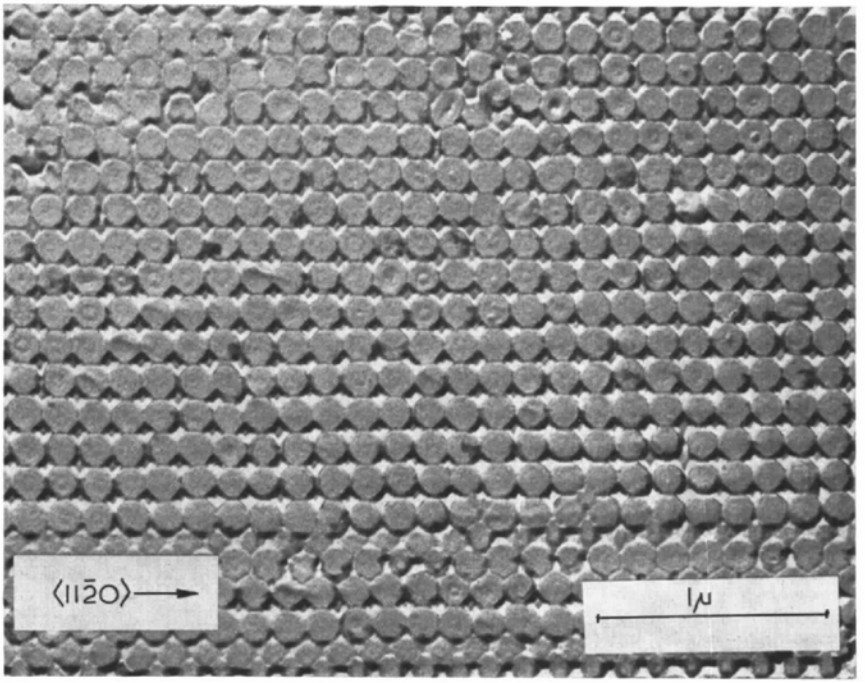

Fig. 11. Electron micrograph of replica of fracture surface of opal showing domain of cubic packing (× 30,000).

[*To face p.* 432

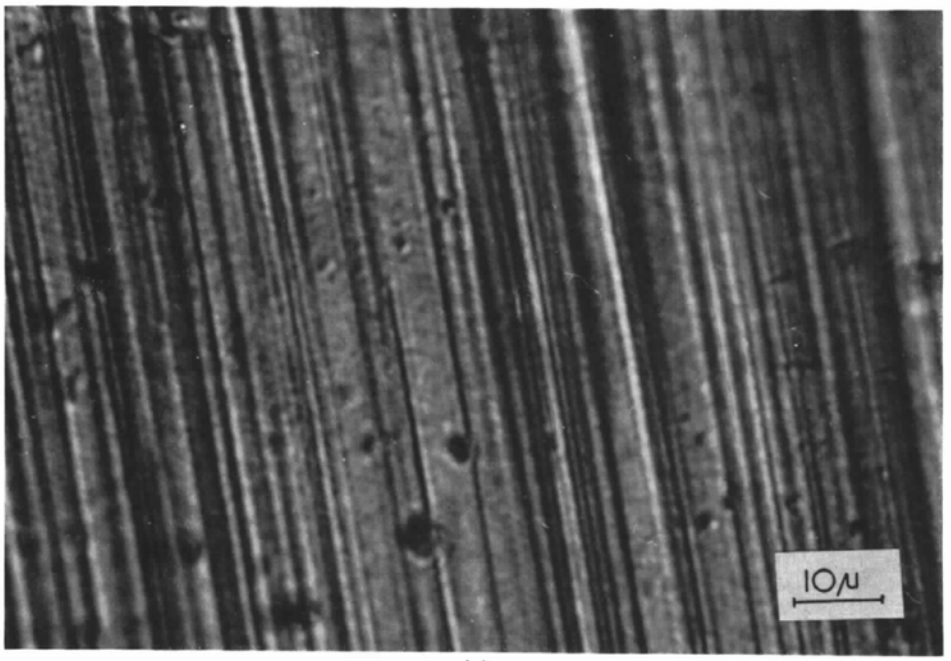

(*a*)

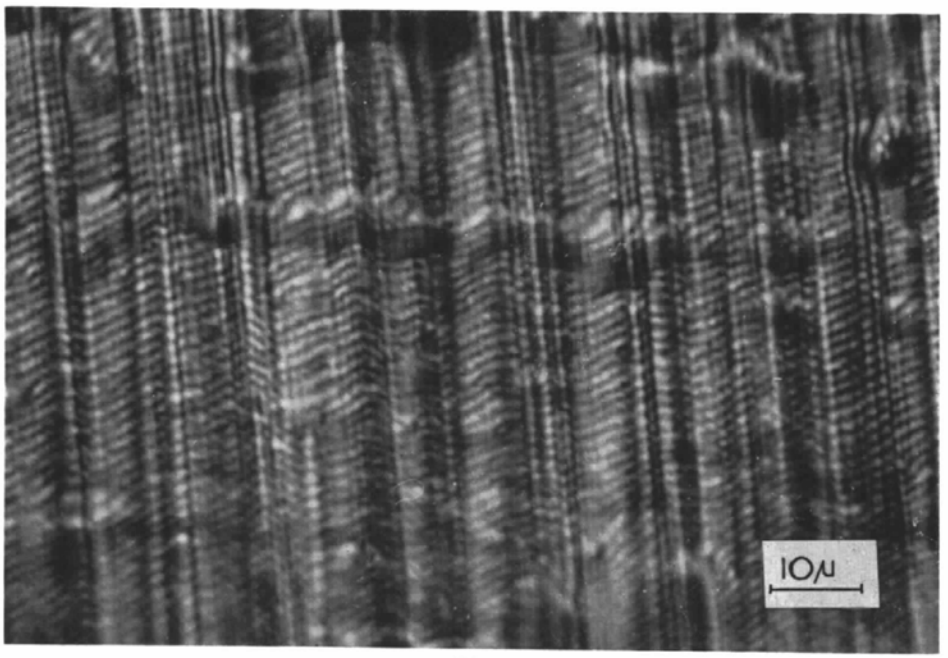

(*b*)

Fig. 12. Optical micrograph of (*a*) bands, and (*b*) fringes from an opal oriented to the position shown in Fig. 10(*a*) (×1200).

main with 12 consecutive layers packed in a regular cubic manner, and bounded by randomly stacked layers on either side. In other sections, up to 30 consecutive layers have been found in a f.c.c. domain.

Optical microscopy

In nearly all precious opal the patches of colour within a grain are traversed by fine parallel straight lines or colourless bands, sometimes visible to the eye but generally requiring a 10× magnifier to be detected. Their complete resolution requires higher magnification and at about 500× the diffracted light can be seen to come from alternate coloured and colourless (black) bands of different widths [Fig. 12(*a*)].

Examination of the various types of opal established that all type I chips contained a set of parallel bands, but that their visibility depended upon the orientation of the chip. When viewed by diffracted light from a pole, no bands were visible. Type IV specimens gave no bands. Type III chips contained two separated, mutually inclined sets, but the boundary between them was not distinguishable.

Some typical chips giving streaks of colour were examined in detail. By tilting specimens and looking at the diffraction streaks by eye in collimated light, it was found that the bands were normal to the reciprocal lattice rod producing the streak of colour. They became most distinct in a metallurgical microscope when the diffracted light was of maximum wavelength, *i.e.* in the orientation sketched in Fig. 10(*a*). Tilting the specimen away from this optimum position about an axis in the surface perpendicular to the streak made the boundaries alternately sharp and diffuse.

A variation of focus produced fringes across the bands, shown in Fig. 12(*b*).

Discussion

The stereograms which have been obtained here from the measurements with the optical diffractometer contain essentially the same features as those described by Baier (1932). However, the interpretation of the stereograms obtained from directly back-diffracted rays is simpler than for other angles of incidence, such as he used.

Here the diffraction patterns and their stereograms have been interpreted with reciprocal lattice geometry by analogy with the X-ray case. The streaks of colour are considered to come from reciprocal lattice rods produced by the disordered stacking of layers of silica particles. It seems more likely that this structure results naturally from the closest packing of the particles of silica settling under the influence of gravity, than from the pseudomorphic replacement of a twinned calcite structure such as Baier (1966) suggested. Darragh, Gaskin, Terrell & Sanders (1965) have suggested a probable mode of formation of opal by the precipitation of silica to form a gel in which primary particles, a few hundred Å in diameter, are produced and then aggregate to produce the spherical particles which pack to make the optical grating. The voids which occur between the particles are a characteristic feature of Australian opals. American opals, although also formed from uniformly sized particles of silica are somewhat different, because no voids can be seen in them (Dietz & Sanders, 1967). However, they give similar diffraction colours and patterns, and it is therefore necessary to postulate that there is nevertheless a regular variation of refractive index associated with the particles.

Although they are generally smaller than the particles in precious opals, large protein molecules and virus particles are well known to order into crystals (Labaw & Wyckoff, 1958). The particles in *tipula iridescent virus*, however, are about the same size as the silica spheres, and their crystals give brilliant diffraction colours (Klug, Franklin & Humphreys-Owen, 1959). Similarly, monodisperse particles of synthetic latex, settling on a flat surface, form a regular array which gives optical diffraction colours (Luck, Klier & Wesslau, 1963). In these last two cases the optical diffraction was consistent with a f.c.c. packing rather than the heavily faulted structure of opals.

The examination of many chips showed that the completely disordered structure is the most common packing arrangement in opals. However, ordering in domains does occur, and over 30 consecutive layers have been observed packed in a non-random manner. The probability of this occurrence by chance is less than $2^{-30} \simeq 10^{-9}$, or once in 300 m of opal, which is much larger than the length scanned. This suggests that there is a bias toward regular packing and implies that there was some interaction between the particles while they were forming into ordered arrays, possibly a charge on the surface produced by the adsorption of water or ionic impurities from the solution in which the silica has been precipitated.

The size of the particles determines the lattice parameter of the grating of voids, and hence the range of colours which can be diffracted. The largest wavelength which appears is that of the directly back-diffracted ray in a streak ($\lambda^s_{\max}$) in the position shown in Fig. 10(*a*). This position corresponds to diffraction from $(10\bar{1}0)$ planes, with a spacing of $r\sqrt{3}$, and hence

$$\lambda^s_{\max} = 2\mu r/\sqrt{3} = 5{\cdot}02r\ .$$

This is larger than the value that was given previously, $\lambda_{\max} = 4{\cdot}74r$ (Sanders, 1964), on the assumption that the colour of maximum wavelength came from diffraction by (111) planes in an unfaulted f.c.c. structure.

From the above relationship, the sizes of the particles in any samples of gem opal can be quickly estimated from visual inspection. In this way gradients of particle size can frequently be detected in opal deposits and commonly the largest particles are found below the smallest, suggesting that differential sedimentation may be important in separating various sizes of particles.

Bernal (1964) and Scott, Charlesworth & Mak (1964) have considered the mechanical packing of hard spheres, and showed how a plane surface can initiate order in vibrating balls. Opal forms in cavities which are frequently parallel sided seams, so that a similar process could operate. Occasional specimens have been found where the fault plane is parallel to the sides of the cavities, but a systematic examination of many specimens showed that the effect is not general, and the fault planes mostly take up random orientations.

The optical micrograph, Fig. 12(*a*), shows a series of grey domains separated by parallel black or white lines. In this sample $\lambda_{max} = 5500$ Å (green), *i.e.* $r = 1100$ Å, and the spacing of the layers is 1800 Å. At the magnification of the micrograph, the layers would appear 0·2 mm apart. The line widths therefore correspond to a few layers, and their separation is between 5 and 20 interlayer distances. Because this image is made from diffracted beams only, the intensities of the bands represent the relative intensities of diffraction from these areas, and therefore the extent of ordering within them. In this orientation [sample set as in Fig. 10(*a*)] the diffracted intensities from domains whose structures were h.c.p., random, or f.c.c. would be expected to decrease in that order. The fringes crossing the bands [Fig. 12(*b*)] are probably Fourier images (Cowley & Moodie, 1957), produced by the diffracted beam passing back through the periodic structure.

In 1845 Sir David Brewster examined opal in an optical microscope and recorded that 'the colours are generally arranged in parallel bands', and deduced 'that the colorific planes or patches consists of minute pores or vacuities arranged in parallel lines . . . to occupy a space in three dimensions' (Brewster, 1845). It seems unlikely that he could have resolved the pore structure of opal, and it is more likely that he saw the fringe pattern [Fig. 12(*b*)] and interpreted it correctly.

I am very grateful for the assistance of Mr D. Pitkethley for carrying out many of the initial measurements and photography. Melbourne jewellers have been very helpful by providing samples of opals, and making gems available for examination.

References

BAIER, E. (1932). *Z. Kristallogr.* A**83**, 141.
BAIER, E. (1966). *Experientia*, **22**, 129.
BERNAL, J. D. (1964). *Proc. Roy. Soc.* A**280**, 299.
BREWSTER, D. (1845). *Edinburgh Phil. J.* **38**, 385.
COWLEY, J. M. & MOODIE, A. F. (1957). *Proc. Phys. Soc.* B**70**, 486.
DARRAGH, P. J., GASKIN, A. J., TERRELL, B. V. & SANDERS, J. V. (1966). *Nature, Lond.* **209**, 13.
DIETZ, R. & SANDERS, J. V. (1967). *Gems & Minerals*, September.
GUINIER, A. (1963). *X-ray Diffraction.* London: Freeman.
JONES, J. B., SANDERS, J. V. & SEGNIT, E. R. (1964). *Nature, Lond.* **204**, 990.
KLUG, A., FRANKLIN, R. E. & HUMPHREYS-OWEN, S. P. F. (1959). *Biochim. Biophys. Acta*, **32**, 203.
LABAW, L. W. & WYCKOFF, R. W. G. (1958). *J. Ultrastructure Research* **2**, 8.
LEECHMAN, F. (1961). *The Opal Book.* Sydney: Ure Smith.
LUCK, W., KLIER, M. & WESSLAU, H. (1963). *Naturwiss.* **50**, 484; *Ber. Bunsenges.* **67**, 75.
RAMAN, C. V. & JAYARAMAN, A. (1953). *Proc. Indian Acad. Sci.* A**38**, 101.
SANDERS, J. V. (1964). *Nature, Lond.* **204**, 1151.
SCOTT, G. D., CHARLESWORTH, A. M. & MAK, M. K. (1964). *J. Chem. Phys.* **40**, 611.

Acta Cryst. (1968). A**24**, 434

An Expression for the Temperature Factor of a Librating Atom

BY E. N. MASLEN

Department of Physics, University of Western Australia, Nedlands, Western Australia

(*Received* 19 *April* 1967 *and in revised form* 14 *August* 1967)

The temperature factor for an atom undergoing librational motion is usually expressed in the form of the Debye–Waller factor appropriate to a translational oscillation with an equivalent root-mean-square amplitude. As a result of this the atomic positions may depart significantly from their true positions, and in an X-ray structure analysis the effect on the final difference density hinders the study of bonding electron distributions. A new form of the temperature factor for thermal librations which obviates these difficulties is proposed.

The Debye–Waller factor (Debye, 1913, 1914) was introduced to account for the effect of translational oscillations, *i.e.* vibrations, on the scattering of X-rays. The original expressions have been generalized to include the effects of anisotropy on this type of thermal motion (Cruickshank, 1956*a*), and these have generally been used as an approximation to describe mixtures of anisotropic translational and librational motions.

The effect of this assumption on the atomic positions from a structure analysis have been investigated by Cruickshank (1956*b*, 1961) and by Busing & Levy (1964). Cruickshank proposed corrections which are